

Synthesis and Characterization of ZnO Doped with Fe₂O₃ — Hydrothermal Synthesis and Calcination Process

D. SIBERA^{a,*}, R. JĘDRZEJEWSKI^a, J. MIZERACKI^b, A. PRESZ^b, U. NARKIEWICZ^a
AND W. ŁOJKOWSKI^b

^aInstitute of Chemical and Environment Engineering, West Pomeranian University of Technology
K. Pułaskiego 10, 70-322 Szczecin, Poland

^bInstitute of High Pressure Physics, Unipress, Polish Academy of Sciences
Sokołowska 29/37, 01-142 Warsaw, Poland

The aim of the present work is to compare two methods of synthesis of nanocrystalline zinc oxide doped with iron oxide. The synthesis was carried out using microwave assisted hydrothermal synthesis and traditional wet chemistry method followed by calcination. The phase composition of the samples was determined using X-ray diffraction measurements. Depending on the chemical composition of the samples, hexagonal ZnO, and/or cubic ZnFe₂O₄ were identified. The morphology of the received materials was characterized using scanning electron microscopy. Two different structures of agglomerates were observed: a hexagonal structure (corresponding to zinc oxide) and spherical (corresponding to spinel phase). The effect of the iron oxide concentration on specific surface area and density of the samples was determined.

PACS numbers: 61.46.-w, 68.37.Hk, 81.07.-b, 81.16.Be

1. Introduction

Zinc oxide is a main component of very interesting and technologically important powder and ceramic materials that have been extensively studied and used for decades. ZnO has a relatively large direct band gap of 3.3 eV at room temperature. Due to its interesting physicochemical properties zinc oxide is a material of wide applications in many fields of industry such as pharmaceutical, ceramics, and rubber production. Recently, it is also considered for spintronics and optoelectronics applications [1–6]. New possible applications of ZnO doped with transition metal (Fe, Mn, Co etc.) are connected with possible ferromagnetic properties at room temperature [7–9]. However, the origin of ferromagnetic behavior in these compounds is not very well known. Recently, it has been shown that the ferromagnetism in these materials can be induced by inclusions of nanoscale oxides of transition metals [10] and/or nanoparticles containing a large concentration of magnetic ions [11]. In the paper [12] it was demonstrated that nano ZnO doped with Mn²⁺ displays a paramagnetic behaviour with a small antiferromagnetic contribution for Mn²⁺ concentrations reaching 10 mol.%. The authors pointed out that lack of ferromagnetism in this material is connected with not clustering of Mn ions during the microwave driven hydrothermal process. The

problem of the origin of ferromagnetical effects in the ZnO:TM (transition metal, TM) compounds remains still open, then it seems to be very important to study a real structure of these materials.

In this work we focused attention on iron doped ZnO, as iron is most common ferromagnetic metal.

2. Experimental

A mixture of iron and zinc hydroxides was obtained by addition of an ammonia solution or 2 M solution of KOH to a 20% solution of a proper amount of Zn(NO₃)₂·6H₂O and Fe(NO₃)₃·4H₂O in water. The obtained hydroxides were filtered, dried and calcined at 300 °C for 1 h. In the hydrothermal synthesis the obtained hydroxides were put in the reactor with microwave emission. The microwave assisted synthesis was conducted under a pressure of 3.8 MPa during 15 min. The obtained product was filtered and dried.

The phase composition of the samples was determined using X-ray diffraction (XRD) (Co K_α radiation, X'Pert Philips). The mean crystallite size of the detected phases was determined using the Scherrer formula. The specific surface area of the nanopowders was determined by the Brunauer–Emmett–Teller (BET) method using the equipment Gemini 2360 of Micromeritics. The helium pycnometer AccuPyc 1330 of Micromeritics was applied to determine the density of powders. The morphology of samples was investigated using scanning electron microscopy (LEO 1530 and Zeiss Supra).

* corresponding author; e-mail: dsibera@zut.edu.pl

3. Results

A high temperature treatment in a classical coprecipitation-calcination synthesis is the main reason of agglomeration of the grains. To avoid this process a low calcination temperature was applied — 300 °C.

In the case of hydrothermal synthesis the formation of agglomerates was minimized because during the hydrothermal process under elevated pressure of 3.8 MPa the synthesis temperature is only 250 °C and the reaction time is short: 15 min. The results of XRD analysis confirmed the proper choice of the synthesis parameters (Figs. 1 and 2).

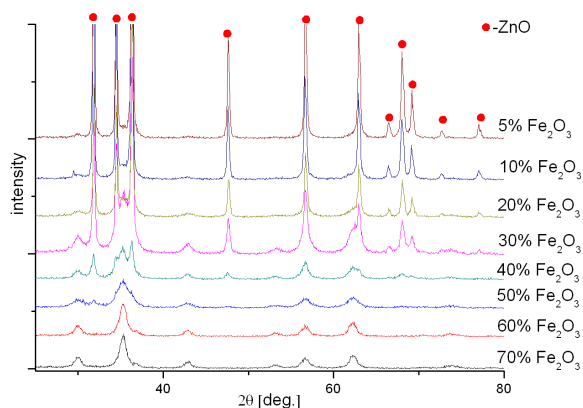


Fig. 1. The XRD patterns of ZnO doped Fe_2O_3 in calcination process. Peaks attributed to ZnO are marked as \bullet . The not marked peaks are attributed to ZnFe_2O_4 .

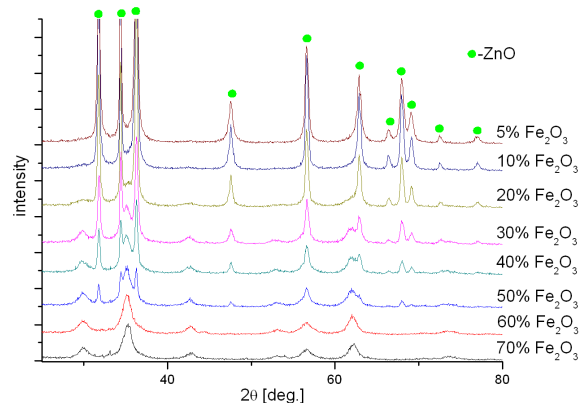


Fig. 2. The XRD patterns of ZnO doped Fe_2O_3 in microwave hydrothermal process. Peaks attributed to ZnO are marked as \bullet . The not marked peaks are attributed to ZnFe_2O_4 .

In the samples obtained using both methods the peaks belonging to ZnO and ZnFe_2O_4 can be found. The intensity of peaks attributed to the spinel increases with increasing Fe_2O_3 content. In both cases up to 20 wt.% Fe_2O_3 no other phases than ZnO are observed. How-

ever, the shape of the peaks is not symmetric and the detailed measurements reveal the presence of small amount of spinel phase. The mean crystallite size of ZnFe_2O_4 , calculated using the Scherrer formula [13], varies from 8 to 12 nm in both methods. In the samples prepared using hydrothermal synthesis the amount of spinel phase is lower comparing with calcination method. For example in the XRD spectrum of the sample containing 50 wt.% Fe_2O_3 in the hydrothermally prepared sample (Fig. 2) the clear peaks attributed to ZnO phase are visible and in case of the same sample prepared by calcination (Fig. 1) the peaks of ZnO phase are much less distinguishable.

The morphology of the samples was investigated using scanning electron microscopy (SEM), see Figs. 3 and 4. Two morphologies can be distinguished — spherical and hexagonal nanograins are observed. We assume the hexagonal crystals correspond to the ZnO, while the small spheroidal crystals — to the ZnFe_2O_4 spinel.

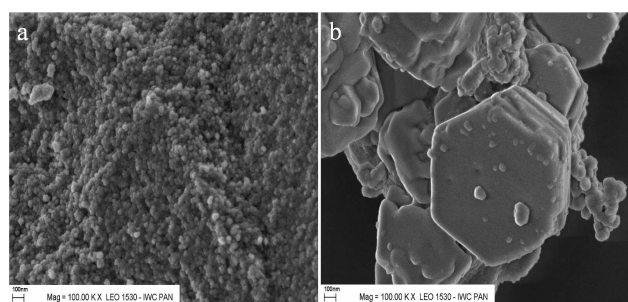


Fig. 3. SEM image of ZnO powders doped in calcination process (a) 70 wt.% Fe_2O_3 , (b) 20 wt.% Fe_2O_3 .

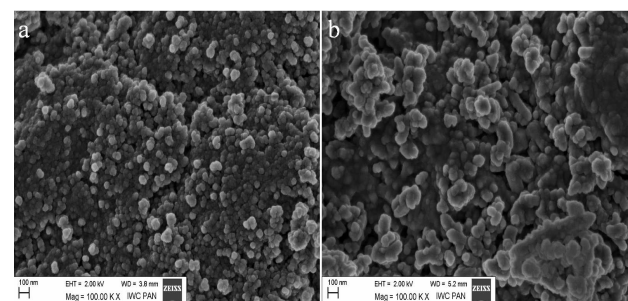


Fig. 4. SEM image of ZnO powders doped in microwave hydrothermal process (a) 70 wt.% Fe_2O_3 , (b) 20 wt.% Fe_2O_3 .

The samples obtained in microwave reactor had considerably larger specific surfaces and smaller density comparing with the samples obtained in calcination process (Table). A density smaller comparing to the calcinated material is connected with the finer grain size. The surface layer of hydroxides may contribute to lower density [14]. It can be explained by a presence of a considerable amount of OH groups on the surface of powders.

TABLE

The results of specific surface area and density measurements.
The accuracy of the measurements was 1%.

Fe ₂ O ₃ [wt.%]	Specific surface area [m ² /g] — microwave hydrothermal process	Specific surface area [m ² /g] — calcination process	Density [g/cm ³] — microwave hydrothermal process	Density [g/cm ³] — calcination process
5	31.1	5.5	5.0	5.3
10	51.1	14.9	5.1	5.2
20	91.9	31.8	5.1	5.1
30	91.4	41.7	4.9	5.1
40	95.5	35.0	4.8	5.2
50	122.5	65.8	4.7	5.0
60	132.3	61.5	4.7	5.0
70	138.7	62.1	4.6	4.9

4. Conclusions

ZnO nanopowders doped with iron oxide contain two crystalline phases: ZnFe₂O₄ and ZnO. In a given sample prepared using hydrothermal synthesis the amount of spinel phase is lower comparing with the same sample synthesised using calcination method. The mean crystallite size of ZnFe₂O₄ varies from 8 to 12 nm with increasing Fe₂O₃ content. The degree of agglomeration of nanopowders depends on the amount of Fe₂O₃ and decreases with increasing Fe₂O₃ content. The specific surface area increases with iron oxide content, contrary to the powder density in both synthesis methods (hydrothermal and coprecipitation-calcination one).

References

- [1] S.J. Pearton, D.P. Norton, K. Ip, Y.W. Heo, T. Steiner, *J. Vac. Sci. Technol. B* **22**, 932 (2004).
- [2] U.Ä. Ozgur, Y. Alivov, C. Liu, A. Teke, M. Reshchikov, S. Dogan, V. Avrutin, S.J. Cho, H. Morko, *J. Appl. Phys.* **98**, 041301 (2005).
- [3] S. Roy, S. Basu, *Bull. Mater. Sci.* **25**, 513 (2002).
- [4] T. Minami, *Mater. Res. Soc. Bull.* **25**, 38 (2000).
- [5] A. Nuruddin, J.R. Abelson, *Thin Solid Films* **394**, 49 (2001).
- [6] J.F. Wager, *Science* **300**, 1245 (2003).
- [7] T. Dietl, H. Ohno, F. Matsukura, J. Cibert, D. Fermand, *Science* **287**, 1019 (2000).
- [8] K.R. Kittilstved, W.K. Liu, D.R. Gamelin, *Nature Mater.* **5**, 291 (2006).
- [9] U. Narkiewicz, D. Sibera, I. Kuryliszyn-Kudelska, L. Kilański, W. Dobrowolski, N. Romcevic, *Acta Phys. Pol. A* **113**, 1695 (2008).
- [10] C. Sudakar, J.S. Thakur, G. Lawes, R. Naik, V.M. Naik, *Phys. Rev. B* **75**, 054423 (2007).
- [11] T. Dietl, *Acta Phys. Pol. A* **111**, 27 (2007).
- [12] A. Tomaszewska-Grzęda, A. Opalińska, E. Grzanka, W. Łojkowski, A. Gedanken, M. Godlewski, S. Yatsunenko, V. Osinniy, T. Story, *Appl. Phys. Lett.* **89**, 242102 (2006).
- [13] P. Scherrer, *Nachr. Ges. Wiss. Göttingen* **2**, 96 (1918).
- [14] *Eight Nanoforum Report: Nanometrology*, Eds. W. Łojkowski, R. Turan, A. Proykova, A. Daniszewska, July 2006.